forests

MDPI

Article

Effects of Salt on Root Aeration, Nitrification, and Nitrogen Uptake in Mangroves

Yan Zhao [1,2,†], Xun Wang [1,3,†], Youshao Wang [1], Zhaoyu Jiang [1,4], Xiaoyu Ma [1,2], Aniefiok Ini Inyang [1] and Hao Cheng [1,*]

1 State Key Laboratory of Tropical Oceanography and Daya Bay Marine Biology Research Station, South China Sea Institute of Oceanology, Chinese Academy of Sciences, Guangzhou 510301, China; zhaoyan1981@qqhru.edu.cn (Y.Z.); kerriganwang@scau.edu.cn (X.W.); yswang@scsio.ac.cn (Y.W.); zyjiang@scsio.ac.cn (Z.J.); 2018906133@qqhru.edu.cn (X.M.); aniefiokinyang@scsio.ac.cn (A.I.I.)
2 College of Life Science and Agroforestry, Qiqihaer University, Qiqihaer 161006, China
3 College of Marine Sciences, South China Agricultural University, Guangzhou 510642, China
4 College of Life Sciences, Linyi University, Linyi 276000, China
* Correspondence: chenghao@scsio.ac.cn
† Authors contributed equally to this work.

Received: 18 October 2019; Accepted: 29 November 2019; Published: 11 December 2019

Abstract: The potential effects of salt on the growth, root anatomy, radial oxygen loss (ROL), and nitrogen (N) dynamics in mangroves were investigated using the seedlings of *Avicennia marina* (Forsk.) Vierh. The results showed that a moderate salinity (200 mM NaCl) appeared to have little negative effect on the growth of *A. marina*. However, higher salt stresses (400 and 600 mM NaCl) significantly inhibited the biomass yield. Concentrations of N in the roots and leaves decreased sharply with increasing salinity. Nevertheless, the presence of salt directly altered root anatomy (e.g., reduced root porosity and promoted suberization within the exodermis and endodermis), leading to a significant reduction in ROL. The results further showed that reduced ROL induced by salt could restrain soil nitrification, resulting in less ammonia-oxidizing archaea and bacteria (AOA and AOB) gene copies and lower concentrations of NO_3^- in the soils. While increased root suberization induced by salt inhibited NH_4^+ and NO_3^- uptake and influx into the roots. In summary, this study indicated that inhibited root aeration may be a defense response to salt, however these root symptoms were not advantageous for rhizosphere nitrification and N uptake by *A. marina*.

Keywords: mangrove; nitrogen; porosity; radial oxygen loss; salt; suberization

1. Introduction

Mangroves are special saline plants that occur in tropical and subtropical costal shores [1–3]. Previous study [4] has reported that potential global warming and sea level rise may further aggravate coastal salinization due to possible increases in saltwater intrusion. Although mangroves are generally considered as salt tolerant plants [5–8], high salinity and excessive salt may inhibit growth of the plants and disturb the nutrient dynamics within mangrove ecosystems [9].

Nitrogen (N) availability is an important limiting factor for the growth, productivity and distribution of mangroves in intertidal regions [10]. In contrast to terrestrial ecosystems, nitrification and micro-formation of NO_3^- in the sediments of mangroves are greatly inhibited [11–14]. Consequently, most inorganic N in mangrove sediments exists in the NH_4^+ form [15–17]. However, Shiau et al. [9] reported that the rates of NO_3^- uptake by the mangrove *Kandelia candel* (L.) Druce were comparable with those of NH_4^+. Previous studies [18,19] have also reported that N acquisition and the productivity of rice are higher under mixed NH_4^+ and NO_3^- sources than NH_4^+ supply alone.

Tidal flooding often results in a shortage of O_2 in the sediments. The successe of mangrove plants is partially attributed to special anatomical structures that enable sufficient O_2 to be supplied to roots [20]. Previous studies [20–22] have reported that most mangroves possess extensive root porosity that provides an internal pathway and benefits O_2 transportation within the roots. During O_2 transportation within the roots, part of the O_2 may leak outside to the rhizosphere sediments simultaneously, a biological process namely radial oxygen loss (ROL) [23–25]. ROL can directly create an aerobic microenvironment around the roots, which is important in restricting an accumulation of potential phytotoxins, and it also benefits aerobic microbial activity, such as for some nitrifying bacteria and archaea [26,27].

ROL is regulated by root aeration and external environments [25,28,29]. Increased root porosities induced by waterlogging have been widely reported [25,29]. Occasionally, wetland plants may evolve an impermeable barrier within the exodermis that prevents ROL from basal and sub-apical roots, while encouraging enough O_2 transfer to the root tips [30,31]. It has been reported that the strength of this barrier is primarily related to the anatomical features of the exodermis (e.g., the thickness of the outer cell layers, and the quantitative variations in suberin deposition) [31]. Such an impermeable barrier would contribute to the formation of an apoplastic transport barrier that influences the fluxes of gases and dissolved ions at the rhizo–root interface [32–34]. Our recent study [35] reported that both salt and N could alter root aeration and ROL in the mangrove *Rhizophora stylosa.* It is of great importance to explore N dynamics in mangroves as affected by salt from the aspect of anatomical adaptation.

This study is, therefore, designed to investigate the relationships among root aeration, ROL, and N dynamics in mangroves. *Avicennia marina* (Forsk.) Vierh is a pioneer mangrove species and widely distributed over tropical and subtropical coastal estuaries. This study elucidates the mechanisms involved in salt tolerance, as well as highlights significant information related to mangrove nutrition.

2. Materials and Methods

2.1. Plant Materials and Preparation

The seeds of *A. marina* were collected from a mangrove wetland located in Gaoqiao, Zhanjiang, China. The seedlings were germinated in sand cultivation beds (approximately 15 cm river sand covered with a thin layer 2 cm of organic peat moss, and irrigated using tap water) under salt-free conditions. The seedlings were and grown in a greenhouse (25 ± 5 °C, 12/12 h day/light cycle, and 300 μmol m^{-2} s^{-1} light intensity) throughout the experiments. Two-month old seedlings with similar size (originally approximately 8 cm in height) were selected as plant materials for the following experiments.

2.2. Experimental Design and Salt Treatments

The objective of the soil pot trial was to evaluate the effects of salt on the N dynamics in the soils in relation to ROL. The pre-cultivated seedlings with similar size, as mentioned above, were carefully taken out from the sand cultivation beds in order to avoid root damage. The seedlings were then transplanted into plastic pots (approximately 18 cm in diameter and 22 cm in height, and 2.6 kg soil per pot) for another two-moth salt exposure. The soil used in the experiment was collected from a wetland park located in Nansha, Guangzhou (particle size: 33% of sand, 45 % of slit and 22% of clay; soil pH: 5.3; soil salinity: 1.5 g kg^{-1}; total N: 1.1 g kg^{-1}; total P: 0.5 g kg^{-1}; and total C: 1.5%). The seedlings were frequently flooded (12/12 h flooded/drained to simulate a 12/12 h high/low tidal cycle) by artificial salty waters containing 0 (control), 200, 400, and 600 mM NaCl, respectively. During the soil pot trial, no N or other nutrients were added. There were 8 pots (4 seedlings per pot) for each salt treatment, and a total of 32 pots were placed in a greenhouse.

A short-term (1 week) solution pot trial was designed to investigate whether and how salt altered the kinetics of NH_4^+ and NO_3^- uptake by the roots of *A. marina* in relation to root suberization. The pre-cultivated seedlings, as mentioned above, were selected and transplanted to pots filled with solutions containing 0 (control), 200, 400, and 600 mM NaCl, respectively. Concentrations of other

elements in the hydroponic systems followed by previous study [36] with modifications: 0.05 mM $(NH_4)_2SO_4$, 0.03 mM $Ca(NO_3)_2$, 0.04 mM KNO_3, 0.025 mM KH_2PO_4, 0.015 mM K_2SO_4, 0.035 mM $MgSO_4$, 55 μM Fe-EDTA, 0.9 μM $MnSO_4$, 2.3 μM H_3BO_3, 0.15 μM $CuSO_4$, and 0.15 μM $ZnSO_4$. There were 16 seedlings for each salt treatment, and a total of 64 seedlings were included in the solution pot trial.

2.3. Plant Growth and Concentrations of N and Na^+ in the Tissues of A. marina

At the end of the salt treatment period, the seedlings were harvested and rinsed carefully with distilled water. Eight seedlings for each salt treatment in the soil pot trial were used for the measurements of plant growth, tissue N and Na^+. Growth parameters, such as seedling height, were detected immediately after harvest. The seedlings were then dried at 60 °C to a constant weight for biomass calculation. The samples of roots and leaves were ground into powder and N contents were determined using a C/N elemental analyzer (Carlo Erba NA 2100, Milan, Italy). As for Na^+ measurement, the samples of roots and leaves were digested by sulphuric acid and hydrogen peroxide, and then analyzed by inductively coupled plasma-optical emission spectrometry (ICP-OES, Optima 7300, Perkin Elmer, Waltham, MA, USA) at 589 nm. Standard materials (GBW-07063, Gsv-2) and blanks were conducted for quality assurance.

2.4. N Dynamics in the Soils

The values of redox potentials (Eh) for the soils around roots (within 2 cm from the seedlings) were detected immediately after harvest. The soils around the roots (approximately sub-surface 2–10 cm in depth, and within 2 cm from the seedlings) were also collected for N analysis. Inorganic N in the soils was extracted using 2 M KCl. Concentrations of nitrate-N(NO_3^--N), nitrite-N (NO_2^--N), and ammonia-N (NH_4^+-N) were then determined using a flow analyzer (QuAAtro39, Seal, Southampton, UK). Nitrification potential activity (NPA) was measured as described by Chen et al. [13]. Briefly, approximately 5 g fresh soil was transferred into a tube and then mixed with 20 ml of artificial seawater containing 10 mM of potassium chlorate, 200 μM of ammonium chloride and 15 μM of sodium phosphate. After incubating in the dark at 25 °C for 48 h, and the concentrations of NO_2^--N were measured using the method as stated above. For each salt treatment, there were 8 replicates for all the detected soil indices.

2.5. Soil DNA Extraction and qPCR Analysis

Quantitative PCR (qPCR) was employed to estimate the abundances of ammonia-oxidizing archaea (AOA) and ammonia-oxidizing bacteria (AOB). Rhizosphere soils, which were sampled by a method of root shaking, collected from four *A. marina* seedlings in each soil pot were mixed as a replicate. There were 8 replicates for each salt treatment, and the abundances of AOA and AOB for each sample were determined in triplicate for qPCR analysis. Soil DNA was extracted using the E.Z.N.A. Soil DNA Kit (OMEGA). The optimized qPCR reaction (25 μL) contained the following reagents: 1 μL DNA (30–50 ng/μL), 12.5 μL SYBR Premix Ex Taq II (TAKARA), 0.5 μL bovine serum albumin (10 mg/mL), 1 μL forward and 1 μL reverse primers (10 μM), and 9 μL ddH_2O. The primers Arch-amoAF (STAATGGTCTGGCTTAGACG) and Arch-amoAR (GCGGCCATCCATCTGTATGT) were used for the amplification of AOA; amoA-1f (GGGGTTTCTACTGGTGGT) and amoA-2r (CCCCTCKGSAAAGCCTTCTTC) were used for the amplification of AOB. The qPCR programs were as follows: AOA: 95 °C for 3 min, 40 cycles of 95 °C for 45 s, 56 °C for 1 min, 72 °C for 1 min; AOB: 95 °C for 3 min, 40 cycles of 95 °C for 45 s, 58 °C for 1 min, 72 °C for 1 min. Plasmid DNA, including cloned PCR amplicons, was extracted using the plasmid extraction (Kit, QMEGA) for qPCR standard curves. Standard curves were constructed using a 10-fold serial dilution of plasmids that contained the corresponding gene sequences. The copy numbers of all of the samples were evaluated and the correlation coefficients (R^2) were higher than 0.98 for the targeted genes.

2.6. The Measurements of ROL and Root Porosity

A root-sleeving O_2 electrode (inner diameter, 1.125 mm) [35] was employed to evaluate the profiles of ROL along laterl roots (n = 8, 8 seedlings for each salt treatment in the soil pot trial, and two lateral roots per seedling were determined and combined as a replicate). The individual seedling was fixed with its roots in a vessel, approximately 1.25 L pre-deoxygenated medium (0.05 % w/v agar) was added into the vessel. The values of ROL were determined at 0.5, 2, and 4 cm from the root tip, respectively. A voltage–current curve without root was also conducted to ensure the medium was deoxygenated absolutely.

For the measurement of ROL from the entire roots, the seedlings (n = 8, 8 seedlings for each salt treatment in the soil pot trial) were transported into a pre-deoxygenated box filled with N_2. The root was immersed in pre-deoxygenated 0.2-strength Hoagland solutions, and then paraffin oil (approximately 2 cm in thickness) was added to minimize re-aeration. Then, 5 mL of titanium (III) citrate stock buffer was added into the solutions. After 24 h of incubation, the changes in the buffers were measured at 527 nm [37]. As for root porosity, a pycnometer method (n = 8, 8 seedlings for each salt treatment in the soil pot trial) was conducted as described by Kludze et al. [37].

2.7. Root Suberization Observation

A photomicroscope equipped with a fluorescence light (Olympus BX 53, Tokyo, Japan) was used for the suberization analysis. Lateral roots with a similar size were selected for the suberization analysis. The roots were frozen at −20 °C together with frozen embedding (colorless Neg-50, Thermo, Waltham, MA, USA). Root sections (0.5, 2, and 4 cm from root tip, respectively) were made by a freezing microtome (Microm HM560-V, Thermo, Waltham, MA, USA). The sections were stained with 0.01% (W/V) fluorol yellow 088 (FY088) (FY088 polyethylene glycol 400—90% glycerol solution, FY088 was dissolved in polyethylene glycol 400, and then an equal amount of 90% glycerol was added into the dye) for 1 hour. After rinsing, the sections were uploaded with 75% glycerol and viewed with UV (excitation 330–385 nm, band barrier >420 nm, green-yellow fluorescence indicated suberization) and field light (for comparison to assist in the suberized cell counting). Root suberization was evaluated based on 8 seedlings per treatment in the solution pot trial. The percentage of biseriate and suberized exodermal layer and suberized endodermal cells were also analyzed.

2.8. The Measurements of NH_4^+ and NO_3^- Fluxes at the Rhizo–Root Interface

The net fluxes of NO_3^- and NH_4^+ at the root surfaces were detected using Non-invasive Micro-test Technology (NMT, NMT100 Series, Younger, Amherst, MA, USA). The NMT analysis has been widely applied for ion flux detection, such as for nutrient ions, gases and heavy metals [38–40]. The microelectrode of $NH4^+$ was manufactured and silanized with NH_4^+-selective liquid cocktail (#09879, Sigma), while NO_3^--selective ion-exchange cocktail (#7254, Sigma) was used in the NO_3^- electrode.

Before NMT analysis, there was a short-term treatment of salt (solution pot trial mentioned above). The fluxes of NO_3^- and NH_4^+ were detected at the apical roots (0.5 cm from the root tip). The selected root position was according to our preliminary experiment; that demonstrated that apical roots exhibited higher nutrient uptake when compared to sub-apical and basal roots. Briefly, the roots were rinsed with distilled water and then incubated in the measuring solution (containing 0.1 mM $CaCl_2$, 0.1 mM KCl, and 0.1 mM NH_4NO_3, pH 5.5) to equilibrate absolutely. The equilibrated roots were then transported to a measuring chamber. The fluxes of ions near the root surface (distance from microelectrode and root was between 5 μm to 35 μm) were detected by moving the ion-selective microelectrode along the roots. For each salt treatment, 4 seedlings were used for the measurement of NO_3^- flux and another 4 seedlings for NH_4^+ analysis. The background was detected by moving the microelectrode in the measuring solution without roots.

2.9. Statistical Analysis

The data were analyzed using SPSS software (version 13.0, Chicago, IL, USA), and all figures were made by PC-based Origin (version 9.0, Hampton, MA, USA). All of the data are presented as mean ± standard deviation. Least significant difference (LSD) and T test were employed to evaluate the differences among the different treatments.

3. Results

3.1. The Effects of Salt on Growth and N Uptake by A. marina

The growth responses of *A. marina* subjected to salt are shown in Table 1. *A. marina* grew normally under the low salt treatment, and no mortality was found even in the highest salt treatment. When compared to the control (irrigated with fresh water), a moderate salinity (200 mM NaCl) appeared to have little negative effect on plant growth. In addition, a higher shoot height was observed in the seedlings irrigated with 200 mM NaCl. However, in the higher salt treatments (400 and 600 mM salt treatments), all growth parameters sharply decreased when compared to the controls (Table 1).

Table 1. Growth parameters of the seedlings of *A. marina* after a 2-month exposure to control, 200, 400, and 600 mM NaCl. The different letters in the same column indicate significant differences at $p < 0.05$.

Salt Treatments (mM NaCl)	Survival (%)	Shoot Height (cm)	No. of Living Leaves	Biomass (g)
Control	100	14.68 ± 1.03 b	8.00 ± 0.82 a	2.28 ± 0.21 a
200	100	16.08 ± 0.16 a	8.75 ± 0.96 a	2.66 ± 0.07 a
400	100	11.65 ± 0.53 c	6.50 ± 1.00 b	1.76 ± 0.09 b
600	100	8.75 ± 0.72 d	6.00 ± 1.63 b	1.32 ± 0.11 c

The concentrations of Na^+ in roots and leaves of *A. marina* increased significantly with rising salinity (Figure 1a). N uptake by plants was also influenced by the external salt addition. The presences of salt directly reduced N accumulations in the plant tissues (Figure 1b).

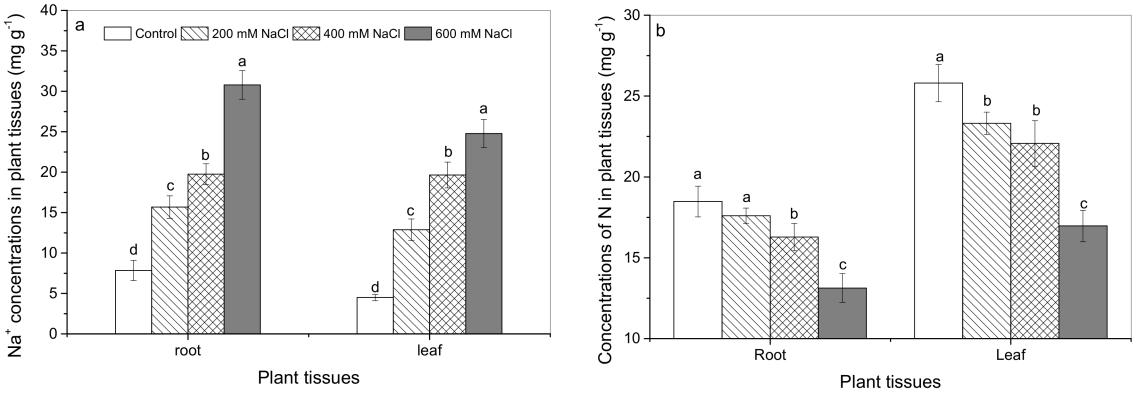

Figure 1. Concentrations of Na^+ (**a**) and total N (**b**) in tissues of *A. marina* after 2-month exposure to control, 200, 400, and 600 mM NaCl. The different letters indicate significant differences at $p < 0.05$.

3.2. The Effects of Salt on ROL and Root Porosity

ROL from roots of *A. marina* decreased significantly when stressed by salt, especially in the apical root regions (Table 2 and Figure 2). In salt-free roots, the values of ROL at apical roots were approximately 40 ng O_2 cm^{-2} min^{-1}. However, in the highest salt treatment, only halfed rates of ROL, approximately 20 ng O_2 cm^{-2} min^{-1}, were detected at apical root regions (Figure 2). When compared to the control roots, decreased root porosity was also detected in the salt-treated seedlings, especially in the higher salt treatments (400 and 600 mM NaCl) (Table 2).

Table 2. Radial oxygen loss (ROL) from entire root ssytems and root porosity in *A. marina* after a 2-month exposure to different salt treatments. The different letters in the same column indicate significant differences at $p < 0.05$.

Salt Treatments (mM NaCl)	Root Porosity (%)	ROL (μmol O_2 d^{-1} g^{-1} Dry Weight $_{root}$)
Control	25.58 ± 1.44 a	30.98 ± 2.50 a
200	24.31 ± 0.81 a	29.75 ± 1.30 a
400	19.24 ± 1.01 b	22.38 ± 0.63 b
600	16.98 ± 0.96 c	18.43 ± 1.63 c

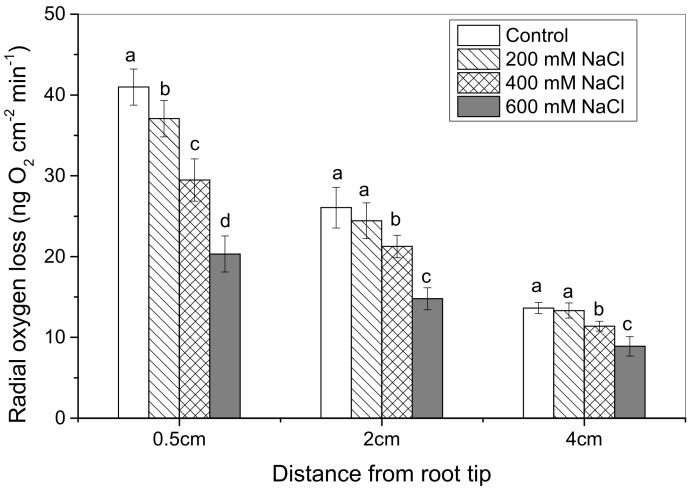

Figure 2. Radial oxygen loss (ROL) from different root regions in *A. marina* after a 2-month exposure to salt. The different letters in the same root position indicate significant differences of ROL rates among salt treatments at $p < 0.05$.

3.3. The Effects of Salt on Root Suberization

The effects of salt on root suberization are shown in Figure 3. The control NaCl-free roots exhibited a uniseriate exodermis with stained suberin lamellae at 0.5 cm from the tip, although suberization was not obvious in some cell walls. At 2 cm from the root tip, the fluorescence intensity increased and some signs of exodermal biseriate thickening were observed. Nearly complete additional exodermal layer with stained suberin (biseriate and suberized exodermal layer, BSEX) was observed at 4 cm from the root tip. When compared to control NaCl-free roots, a promotion in suberization (e.g., increased BSEX formation induced by salt) was observed in the exodermis of the salt treated roots. In addition, the formation of BSEX began closer to the root tip, and the effects became more pronounced when stressed by the highest salt treatment 600 mM NaCl. Similar to suberization within the exodermis, increased suberization induced by salt was also observed within the endodermal cell walls.

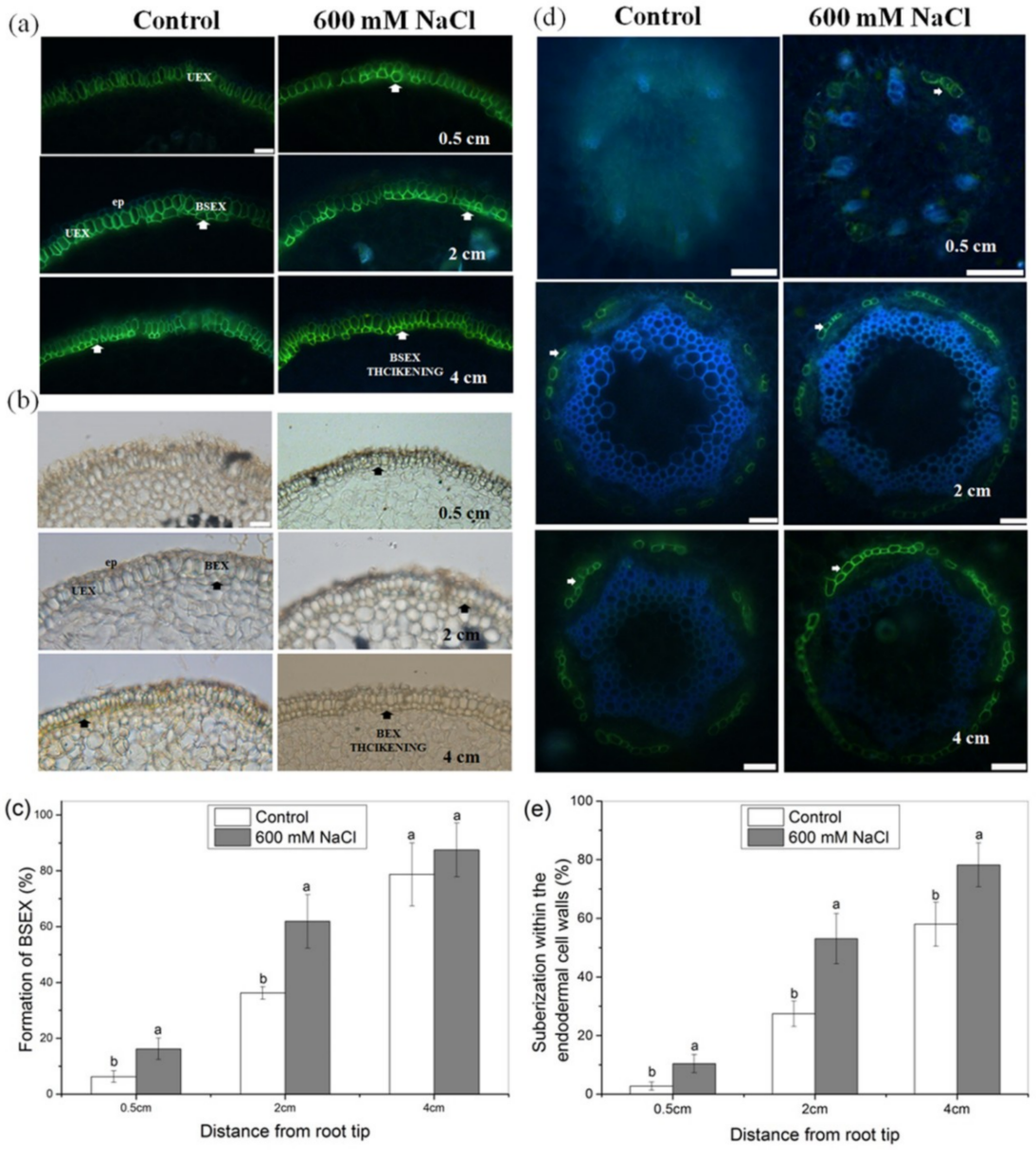

Figure 3. Root suberization in *A. marina* subjected to salt. Root sections (0.5, 2, and 4 cm from root the tip, bar = 50 μm) made from control and salt treated (600 mM NaCl for 1 week) roots. (**a**) Suberization within the exodermis, green-yellow fluorescence indicated suberization, and the formation of biseriate and suberized exodermis (BSEX) is highlighted with the arrows. (**b**) Characteristics of outer cell layers and the formation of the second additional exodermis. (**d**) Suberization within endodermis is shown in figure, and the arrows indicate the deposition of suberin within endodermal cell walls. The statistical analysis of suberization within the exodermis (**c**) and the endodermis (**e**), $n = 8$, the different letters indicate significant differences between treatments at $p < 0.05$. The abbreviations in the figures are the following: BEX: biseriate exodermis; BSEX: biseriate and suberized exodermis; UEX: uniseriate exodermis; ep: epidermis.

3.4. The Effects of Salt on N Dynamics in the Soils Planted with A. marina

The effects of salt on N dynamics in soils were illustrated in Figure 4. Soil NH_4^+ appears to exhibit no significant differences among the various salt treatments (Figure 4a). The concentrations of NO_3^-, however, were found to be influenced by salt. When compared to controls, lower concentrations of of NO_3^- were detected in the soils under salt treatments, especially in the higher salt treatments (400 and

600 mM NaCl) (Figure 4b). Similarly, the significant reductions in soil Eh, nitrification, AOA and AOB gene copies induced by salt (e.g., 400 and 600 mM NaCl) were also observed (Figure 4c–f).

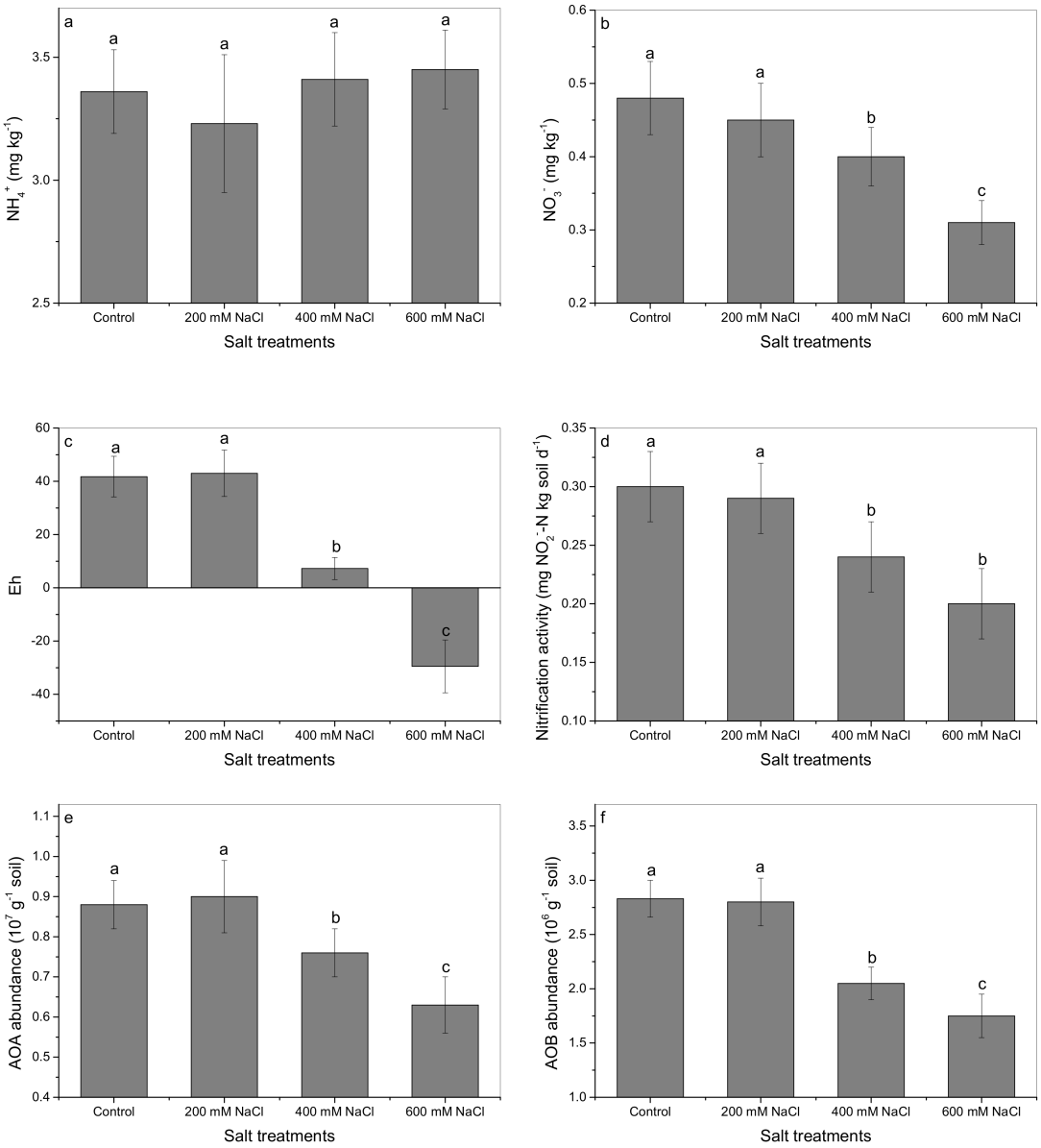

Figure 4. The effects of salt on N dynamics and microenvironment in soils planted with *A. marina*. (**a**) NH_4^+ concentrations. (**b**) NO_3^- contents. (**c**) Soil redox potentials. (**d**) Nitrification activity. The abundances of AOA (**e**) and AOB (**f**). The different letters indicate significant differences among salt treatments at $p < 0.05$.

3.5. The Effects of Salt on NH_4^+ and NO_3^- Fluxes at the Rhizo–Root Interface

The fluxes of NH_4^+ and NO_3^- at the rhizo–root interface are shown in Figure 5. The influxes of NH_4^+ and NO_3^- in the control roots were 82.66 pmol cm^{-2} s^{-1} and 74.58 pmol cm^{-2} s^{-1}, respectively, indicating that the absorption and utilization of NH_4^+ and NO_3^- by *A. marina* were comparable. Both the NH_4^+ and NO_3^- influxes decreased significantly when stressed by salt.

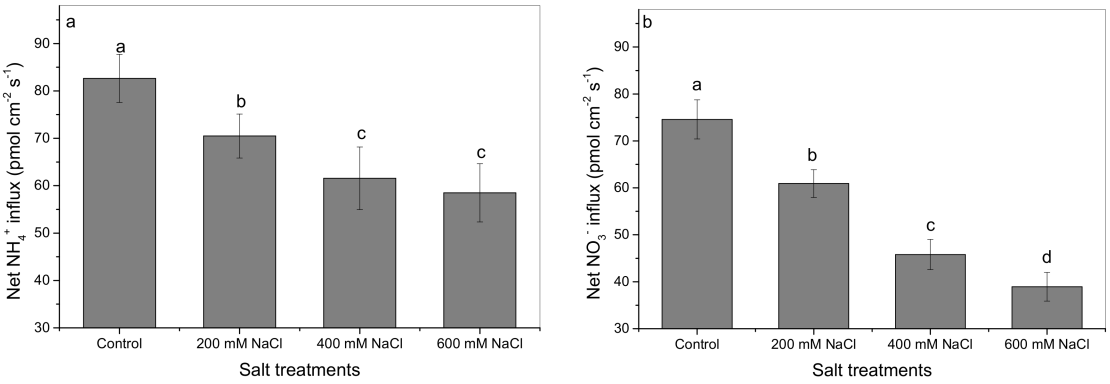

Figure 5. Fluxes of NH_4^+ (**a**) and NO_3^- (**b**) at the root surface in *A. marina* as affected by salt. The different letters indicate significant differences among salt treatments at $p < 0.05$.

4. Discussion

4.1. Growth and N Uptake by A. marina under Elevated Salinity

Despite the importance of mangrove, it is a sensitive and fragile ecosystem that is threatened by both human activities and global climate changes. The results of this study showed that a moderate salinity (200 mM NaCl) appeared to have little negative effect on the growth of *A. marina*. However, higher salt stresses (400 and 600 mM NaCl) directly inhibited biomass yield and N uptake (Table 1, Figure 1). Previous studies [41–43] have also claimed that the optimal salinity for mangroves is approximately 25%–50% natural seawater (approximately 140–280 mM NaCl). Hence, a high salinity would not benefit mangrove growth and productivity. *A. marina* is one of the most salt tolerant mangrove species, and salt induced inhibition may be more serious in other mangrove species. More detailed researches and long-term observations that focus on the responses of mangroves to potential salinity changes need to be conducted. Additionally, it has been reported that potential global warming and sea level rise may aggravate coastal salinization [4]. The implications of this study would be helpful for estimating the response of mangroves to potential global warming and salinity changes.

It should be noted that the influences of salt on plant growth did not absolutely coincided with N uptake. In the soil pot trial, growth inhibitions were only observed in the higher salt treatments (400 and 600 mM NaCl); whereas concentrations of total N in the tissues of *A. marina* sharply declined with elevated salinity. The results from NMT also showed that the presence of salt directly reduced NH_4^+ and NO_3^- uptake by *A. marina* (Figure 5). Patel et al. [43] found that the growth of *A. marina* was significantly promoted by low salinity; however, the concentrations of K, Ca, Mg, and N decreased significantly. All of these data indicated that *A. marina* may possess some mechanisms that maintain growth and productivity under a moderate salt stress, whereas N acquisition is restrained. It has been [44] reported that low salinity can promote the activities of nitrate reductase, acid phosphatase and alkaline phosphatase in *Bruguiera parviflora*, which may partially alleviate nutrient metabolism under salt stresses. Antioxidant systems [45,46], salt secretion [34,47], and nutrient re-sorption [48] may also benefit plant growth and alleviate salt induced inhibition.

4.2. The Effects of Salt on Root Anatomy and ROL

The present study (Table 2 and Figure 2) showed that salt can directly inhibit ROL from roots. ROL in apical roots were more sensitive to the external salinity. The values of ROL at 0.5 cm from root tip were significantly inhibited when treated by salt, even in the lowest salt treatment (200 mM NaCl). Similar reductions in ROL induced by heavy metals were also reported by previous study [49].

Reduced ROL stressed by salt was mainly ascribed to the alterations in root aeration [30,31,50]. Aerenchyma provides a low resistance internal pathway for gas diffusion within the roots [25,51]. However, the results of this study (Table 2) clearly showed that salt significantly reduced root

porosity and inhibited the formation of aerenchyma. A reduced root porosity induced by salt may block the longitudinal transport of O_2 within the roots, causing less O_2 arrival to roots and/or the rhizosphere. Moreover, the photos presented in Figure 3 primarily illustrated the effects of salt on root anatomy in *A. marina* (e.g., suberization thickening within the exodermal and endodermal cell walls). Krishnamurthy et al. [34] also reported that salt could promote suberin deposition within the roots of *Avicennia officianalis*. Generally, suberin deposition within the outer cell layers was considered as a major barrier to ROL [31]. The promotion of suberization within the exodermis induced by salt could directly promote the resistance of O_2 transverse diffusion from inside roots to outside rhizosphere and impede ROL sufficiently.

Recently, some possible molecular mechanisms involved in aerenchyma formation and suberin biosynthesis were confirmed in model plants. Aerenchyma formation may be related to programmed cell death, and regulated by ethylene and reactive oxygen (ROS) [49,52,53]. Suberin is a heterogeneous biopolymer composed of aromatic and aliphatic domains (e.g., carboxylic acids, ω− hydroxyacids, diacids, ferulic acids and coumaric acids) [54]. The hypothetical pathway for suberin biosynthesis may be related to precursor synthesis (e.g., Cytochrome P450 monooxygenase, 3-ketoacyl-CoA synthase, fatty acid elongase and acyltransferase), transportation (e.g., ATP-binding cassette transporter transporters) and polymerization (e.g., Class III peroxidase) [55–57]. Due to a lack of genetic information for mangroves, only Krishnamurthy et al [34] reported the role of P450 (CYP86A1) in suberin deposition in the roots of *Avicennia officinalis*. More similar studies that focus on mangroves (e.g., aerenchyma development, suberin biosynthesis, and as well as the correlations between these two biological processes) need to be conducted.

4.3. N Uptake by A. marina Stressed by Salt in Relation to ROL and Root Suberzation

The present study clearly illustrated that the reduction in N uptake induced by salt coincided with decreased ROL (Table 2, Figures 1 and 2). Reef et al. [10] has claimed the importance of ROL in mangrove nutrition and speculated that ROL is one of the important reasons contributing to high productivity in mangroves. It has been accepted that the sediments in mangroves are often anaerobic due to tidal flooding, and most inorganic N exists in the NH_4^+ form. However, the results of this study (Figure 5) showed that *A. marina* could take up both NO_3^- and NH_4^+ at a similar rate. Similar results were also found in *Kandelia candel* [9]. Some other lab experiments also claimed that the presence of NO_3^- could promote N acquisition and use efficiency by rice [18,19]. ROL from roots could directly oxidize some potential flooding induced phytotoxins (e.g., H_2S, S^{2-}, and CH_4) in the rhizosphere [5]. Moreover, ROL from roots could benefit the activities of nitrification prokaryotes and the micro-formation of NO_3^-, which would contribute nutrition absorption and assimilation by wetland plants [26]. In this study, the reduced ROL induced by salt may aggravate phytotoxic accumulation, leading to an extra inhibition of growth. More importantly, the reduction in ROL induced by salt could restrain soil nitrification and AOA/AOB activities, leading to less micro-formation of NO_3^- (Figure 4). To our best knowledge, this is the first attempt to explore the effects of salt on N dynamics in mangroves from the aspect of root aeration and ROL.

The present results (Figure 3) also showed that salt could directly promote root suberization both in the exodermal and endodermal cell layers. Similar suberization and/or lignification thickening were also reported when plants were exposed to excess heavy metals [58], sulfide [59], and organic acids [60]. All of these symptoms have been defined as a barrier security function to prevent further ingress of toxins into the roots [34,61,62]. However, this impermeable barrier may be not advantageous to nutrient uptake by plants. The data of NMT (Figure 5) clearly showed that both the NH_4^+ and NO_3^- influxes were inhibited in salt treated roots when compared to controls.

Our previous study [35] reported that the mangrove *Rhizophora stylosa* appeared to promote root aeration (e.g., increasing root porosity and reducing root lignification simultaneously) under N deficiency conditions. A similar promotion in root aeration induced by N deficiency has also been found in *Ricinus communis* [63], rice [64] and maize [65]. Here as a strategy that the roots with high

aeration (e.g., a thin exodermis with low suberization together with extensive porosity and powerful ROL) can be speculated to promote soil nitrification and N uptake by mangroves. Pi et al. [21] and our previous study [22,58] reported that ROL and root anatomy varied significantly among different mangrove species. It is interesting to further compare N uptake and utilization among different mangrove species in relation to root aeration and ROL.

5. Conclusions

The results showed that high salinity directly increased suberization both in the exodermis and endodermis, leading to significant reductions in ROL from the roots of *A. marina*. Reduced root porosity stressed by salt also contributed to less ROL. Moreover, these root symptoms could regulate the N dynamics both in the rhizosphere and at the rhizo–root interface. Coinciding with reduced root aeration and ROL, decreased soil nitrification, AOA and AOB gene copies, and as well as an obvious reduction in biomass yield and NH_4^+ and NO_3^- uptake by *A. marina* were also observed. The results of this study indicated that inhibited root aeration may be a defense response to salt. However, these root symptoms were not advantageous for rhizosphere nitrification and N uptake by *A. marina*. The implications of this study not only elucidate the mechanisms involved in salt tolerance and mangrove nutrition, but they also highlight information that is very significant for evaluating the responses of mangroves to potential global warming and salinity changes.

Author Contributions: Y.Z. and X.W. conducted the experiments. Z.J. helped in N analysis. X.M. helped in the measurement of root anatomy. A.I.I. and Y.W. contributed in manuscript revision. H.C. supervised the experiments.

Funding: This research was supported by the National Natural Science Foundation of China (Nos. 41676086, 41430966), Science and Technology Basic Resources Investigation Program of China (2017FY100707), Natural Science Foundation of Guangdong province (2014A030313783), Science and Technology Project of Guangdong province (2016A020222011), Guangdong special branch plans young talent with scientific and technological innovation (2016TQ03Z985), Guangzhou Science and Technology Project (20171001013) and The program of preponderant and characteristic discipline of Heilong Jiang province (YSTSXK201879).

Acknowledgments: Thanks to Renjiang Chen for his help during the experiments. We sincerely thank Letpub for its linguistic assistance and the anonymous reviewers for their suggestive comments.

Conflicts of Interest: The authors declare no conflict of interest associated with this publication.

References

1. Wang, W.Q.; Li, X.F.; Wang, M. Propagules dispersal determines mangrove zonation at intertidal and estuarine scales. *Forests* **2019**, *10*, 245. [CrossRef]
2. Alongi, D.M. Present state and future of the world's mangrove forests. *Environ. Conserv.* **2002**, *29*, 331–349. [CrossRef]
3. Ranjan, P.; Ramanathan, A.L.; Kumar, A.; Singhal, R.K.; Datta, D.; Venkatesh, M. Trace metal distribution, assessment and enrichment in the surface sediments of Sundarban mangrove ecosystem in India and Bangladesh. *Mar. Pollut. Bull.* **2018**, *127*, 541–547. [CrossRef] [PubMed]
4. Ranjan, S.P.; Kazama, S.; Sawamoto, M. Effects of climate and land use changes on groundwater resources in coastal aquifers. *J. Environ. Manag.* **2006**, *80*, 25–35. [CrossRef] [PubMed]
5. Clark, D.A.; Brown, S.; Kicklighter, D.W.; Chambers, J.Q.; Thomlinson, J.R.; Ni, J.; Holland, E.A. Net primary production in tropical forests: An evaluation and synthesis of existing field data. *Ecol. Appl.* **2001**, *11*, 371–384. [CrossRef]
6. Zheng, W.J.; Wang, W.Q.; Lin, P. Dynamics of element contents during the development of the hypocotyles and leaves of certain mangrove species. *J. Exp. Mar. Biol. Ecol.* **1999**, *233*, 247–257. [CrossRef]
7. Parida, A.K.; Jha, B. Salt tolerance mechanisms in mangroves: A review. *Trees* **2010**, *24*, 199–217. [CrossRef]
8. Jiang, G.F.; Goodale, U.M.; Liu, Y.Y.; Hao, G.Y.; Cao, K.F. Salt management strategy defines the stem and leaf hydraulic characteristics of six mangrove tree species. *Tree Physiol.* **2017**, *37*, 289–401. [CrossRef]
9. Shiau, Y.J.; Lee, S.C.; Chen, T.H.; Tian, G.L.; Chiu, C.Y. Water salinity effects on growth and nitrogen assimilation rate of mangrove (Kandelia candel) seedlings. *Aquat. Bot.* **2017**, *137*, 50–55. [CrossRef]
10. Reef, R.; Feller, I.C.; Lovelock, C.E. Nutrition of mangroves. *Tree Physiol.* **2010**, *30*, 1148–1160. [CrossRef]

11. Feller, I.C.; McKee, K.L.; Whigham, D.F.; O'Neill, J.P. Nitrogen vs. phosphorus limitation across an ecotonal gradient in a mangrove forest. *Biogeochemistry* **2003**, *62*, 145–175. [CrossRef]
12. Lin, Y.M.; Liu, X.W.; Zhang, H.; Fan, H.Q.; Lin, G.H. Nutrient conservation strategies of a mangrove species Rhizophora stylosa under nutrient limitation. *Plant Soil* **2010**, *326*, 469–479. [CrossRef]
13. Chen, J.; Zhou, H.C.; Pan, Y.; Shyla, F.S.; Tam, N.F.Y. Effects of polybrominated diphenyl ethers and plant species on nitrification, denitrification and anammox in mangrove soils. *Sci. Total Environ.* **2016**, *553*, 60–70. [CrossRef]
14. Alongi, D.M. Impact of global change on nutrient dynamics in mangrove forests. *Forests* **2018**, *9*, 596. [CrossRef]
15. Inoue, T.; Nohara, S.; Takagi, H.; Anzai, Y. Contrast of nitrogen contents around roots of mangrove plants. *Plant Soil* **2011**, *399*, 471–483. [CrossRef]
16. Wang, Y.F.; Gu, J.D. Higher diversity of ammonia/ammonium-oxidizing prokaryotes in constructed freshwater wetland than natural coastal marine wetland. *Appl. Microbiol. Biotechnol.* **2013**, *97*, 7015–7033. [CrossRef]
17. Xiao, K.; Wu, J.P.; Li, H.L.; Hong, Y.G.; Wilson, A.M.; Jiao, J.J.; Shananan, M. Nitrogen fate in a subtropical mangrove swamp: Potential association with seawater-groundwater exchange. *Sci. Total Environ.* **2018**, *635*, 586–597. [CrossRef]
18. Raman, D.R.; Spanswick, R.M.; Walker, L.P. The kinetics of nitrate uptake from lowing nutrient solutions by rice: Influence of pretreatment and light. *Bioresour. Technol.* **1995**, *53*, 125–132. [CrossRef]
19. Kronzucker, H.J.; Siddiqi, M.Y.; Glass, A.D.M.; Kirk, G.J.D. Nitrate-ammonium synergism in rice: A subcellular flux analysis. *Plant Physiol.* **1999**, *119*, 1041–1046. [CrossRef]
20. Youssef, T.; Saenger, P. Anatomical adaptive strategies to flooding and rhizosphere oxidation in mangrove seedlings. *Aust. J. Bot.* **1996**, *44*, 297–313. [CrossRef]
21. Pi, N.; Tam, N.F.Y.; Wu, Y.; Wong, M.H. Root anatomy and spatial pattern of radial oxygen loss of eight true mangrove species. *Aquat. Bot.* **2009**, *90*, 222–230. [CrossRef]
22. Cheng, H.; Wang, Y.S.; Fei, J.; Jiang, Z.Y.; Ye, Z.H. Differences in root aeration, iron plaque formation and waterlogging tolerance in six mangroves along a continues tidal gradient. *Ecotoxicology* **2015**, *242*, 1659–1667. [CrossRef]
23. Armstrong, W. Radial oxygen losses from intact rice roots as affected by distance from apex, respiration and waterlogging. *Plant Physiol.* **1971**, *25*, 192–197. [CrossRef]
24. Armstrong, W.; Beckett, P.M. Internal aeration and the development of stelar anoxia in submerged roots: A multishelled mathematical model combining axial diffusion of oxygen in the cortex with radial losses to the stele, the wall layers and the rhizosphere. *New Phytol.* **1987**, *105*, 221–245. [CrossRef]
25. Colmer, T.D.; Pedersen, O. Oxygen dynamics in submerged rice (Oryza sativa). *New Phytol.* **2008**, *178*, 326–334. [CrossRef] [PubMed]
26. Li, Y.L.; Fan, X.R.; Shen, Q.R. The relationship between rhizosphere nitrification and nitrogen-use efficiency in rice plants. *Plant Cell Environ.* **2008**, *31*, 73–85. [CrossRef] [PubMed]
27. Phukan, U.J.; Mishra, S.; Shukla, R.K. Waterlogging and submergence stress: Affects and acclimation. *Crit. Rev. Biotechnol.* **2016**, *36*, 956–966. [CrossRef]
28. Evans, D.E. Aerenchyma formation. *New Phytol.* **2003**, *161*, 35–49. [CrossRef]
29. Colmer, T.D. Long-distance transport of gases in plants: A perspective on internal aeration and radial loss from roots. *Plant Cell Environ.* **2003**, *26*, 17–36. [CrossRef]
30. Soukup, A.; Armstrong, W.; Schreiber, L.; Franke, R.; Votrubová, O. Apoplastic barriers to radial oxygen loss and solute penetration: A chemical and functional comparison of the exodermis of two wetland species, Phragmites australis and Glyceria maxima. *New Phytol.* **2007**, *173*, 264–278. [CrossRef]
31. Garthwaite, A.J.; Armstrong, W.; Colmer, T.D. Assessment of O_2 diffusivity across the barrier to radial O_2 loss in adventitious roots of Hordeum marinum. *New Phytol.* **2008**, *179*, 405–416. [CrossRef] [PubMed]
32. Degenhardt, B.; Gimmler, H. Cell wall adaptations to multiple environmental stresses in maize roots. *Plant Cell Environ.* **2000**, *51*, 595–603. [CrossRef] [PubMed]
33. Pollard, M.; Beisson, F.; Li, Y.H.; Ohlrogge, J.B. Building lipid barriers: Biosynthesis of cutin and suberin. *Trends Plant Sci.* **2008**, *13*, 236–246. [CrossRef]
34. Krishnamurthy, P.; Jyothi-Prakash, P.A.; Qin, L.; He, J.; Lin, Q.S.; Loh, C.S.; Kumar, P.P. Role of hydrophobic barriers in salt exclusion of a mangrove plant Avicennia officinalis. *Plant Cell Environ.* **2014**, *37*, 1656–1671. [CrossRef]

35. Cheng, H.; Wang, Y.S.; Ye, Z.H.; Chen, D.T.; Wang, Y.T.; Peng, Y.L.; Wang, L.Y. Influence of N deficiency and salinity on metal (Pb, Zn and Cu) accumulation and tolerance by *Rhizophora stylosa* in relation to root anatomy and permeability. *Environ. Pollut.* **2012**, *164*, 110–117. [CrossRef]
36. Miyamoto, N.; Steudle, E.; Hirasawa, T.; Lafitte, R. Hydraulic conductivity of rice roots. *J. Exp. Bot.* **2001**, *52*, 1835–1846. [CrossRef]
37. Kludze, H.K.; DeLaune, R.D.; Patrick, W.H. Aerenchyma formation and methane and oxygen exchange in rice. *Soil Sci. Soc. Am. J.* **1993**, *57*, 386–391. [CrossRef]
38. Brundrett, M.C.; Kendrick, B.; Peterson, C.A. Efficient lipid staining in plant material with Sudan red 7B or Fluorol yellow 088 in polyethylene glycol-glycerol. *Biotech. Histochem.* **1991**, *66*, 111–116. [CrossRef]
39. Luo, J.; Li, H.; Liu, T.X.; Polle, A.; Peng, C.H.; Luo, Z.B. Nitrogen metabolism of two contrasting poplar species during acclimation to limiting nitrogen availability. *J. Exp. Bot.* **2013**, *64*, 4207–4224. [CrossRef]
40. Hawkins, B.J.; Robbins, S.; Proter, R.B. Nitrogen uptake over entire root systems of tree seedlings. *Tree Physiol.* **2014**, *34*, 334–342. [CrossRef]
41. Downton, W.J.S. Growth and osmotic relations of the mangrove *Avicennia marina*, as influenced by salinity. *Aust. J. Plant Physiol.* **1982**, *9*, 519–528. [CrossRef]
42. Burchett, M.D.; Clarke, C.J.; Field, C.D.; Pulkownik, A. Growth and respiration in two mangrove species at a range of salinities. *Physiol. Plant* **1989**, *75*, 299–303. [CrossRef]
43. Patel, N.T.; Gupta, A.; Pandey, A.N. Salinity tolerance of *Avicennia marina* (Forssk.) Vierh. from Gujarat coasts of India. *Aquat. Bot.* **2010**, *93*, 9–16. [CrossRef]
44. Parida, A.K.; Das, A.B. Effects of NaCl stress on nitrogen and phosphorous metabolism in a true mangrove Bruguiera parviflora grown under hydroponic culture. *J. Plant Physiol.* **2004**, *161*, 921–928. [CrossRef] [PubMed]
45. Hossain, M.D.; Inafuku, M.; Iwasaki, H.; Taira, N.; Mostofa, M.G.; Oku, H. Differential enzymatic defense mechanisms in leaves and roots of two true mangrove species under long-term salt stress. *Aquat. Bot.* **2017**, *142*, 32–40. [CrossRef]
46. Lv, X.B.; Li, D.H.; Yang, X.B.; Zhang, M.W.; Deng, Q. Leaf enzyme and plant productivity responses to environmental stress associated with sea level rise in two Asian mangrove species. *Forests* **2019**, *10*, 250. [CrossRef]
47. Chen, J.A.; Xiao, Q.A.; Wu, F.H.; Dong, X.J.; He, J.X.; Pei, Z.M.; Zheng, H.L. Nitric oxide enhances salt secretion and Na^+ sequestration in a mangrove plant, Avicennia marina, through increasing the expression of H^+-ATPase and Na^+/H^+ antiporter under high salinity. *Tree Physiol.* **2010**, *30*, 1570–1585. [CrossRef]
48. Wang, W.Q.; You, S.Y.; Wang, Y.B.; Huang, L.; Wang, M. Influence of frost on nutrient resorption during leaf senescence in a mangrove at its latitudinal limit of distribution. *Plant Soil* **2011**, *342*, 105–115. [CrossRef]
49. Cheng, H.; Tam, N.F.Y.; Wang, Y.S.; Li, S.Y.; Chen, G.Z.; Ye, Z.H. Effect of copper on growth, radial oxygen loss and root permeability of seedlings of the mangroves Bruguiera gymnorrhiza and Rhizophora stylosa. *Plant Soil* **2012**, *359*, 255–266. [CrossRef]
50. Xu, Q.T.; Yang, L.; Zhou, Z.Q.; Mei, F.Z.; Qu, L.H.; Zhou, G.S. Process of aerenchyma formation and reactive oxygen species induced by waterlogging in wheat seminal roots. *Plant Soil* **2013**, *238*, 969–982. [CrossRef]
51. Dai, M.Y.; Liu, J.C.; Liu, W.W.; Lu, H.L.; Jia, H.; Hong, H.L.; Yan, C.L. Phosphorus effects on radial oxygen loss, root porosity and iron plaque in two mangrove seedlings under cadmium stress. *Mar. Pollut. Bull.* **2017**, *119*, 262–269. [CrossRef]
52. Yoo, Y.H.; Choi, H.K.; Jung, K.H. Genome-wide identification and analysis of genes associated with lysigenous aerenchyma formation in rice roots. *J. Plant Biol.* **2015**, *58*, 117–127. [CrossRef]
53. Yamauchi, T.; Colmer, T.D.; Pedersen, O.; Nakazono, M. Regulation of root traits for internal aeration and tolerance to soil waterlogging-flooding stress. *Plant Physiol.* **2018**, *176*, 118–1130. [CrossRef]
54. Cheng, H.; Jiang, Z.Y.; Liu, Y.; Ye, Z.H.; Wu, M.L.; Sun, C.C.; Sun, F.L.; Fei, J.; Wang, Y.S. Metal (Pb, Zn and Cu) uptake and tolerance by mangroves in relation to root anatomy and lignification/suberization. *Tree Physiol.* **2014**, *34*, 646–656. [CrossRef]
55. Kulichikhin, K.; Yamauchi, T.; Watanabe, K.; Nakazono, M. Biochemical and molecular characterization of rice (*Oryza sativa* L.) roots forming a barrier to radial oxygen loss. *Plant Cell Environ.* **2014**, *37*, 2406–2420. [CrossRef]

56. Kotula, L.; Schreiber, L.; Colmer, T.D.; Nakazono, M. Anatomical and biochemical characterisation of a barrier to radial O_2 loss in adventitious roots of two contrasting *Hordeum marinum* accessions. *Funct. Plant Biol.* **2017**, *44*, 845–857. [CrossRef]
57. Shiono, K.; Yamauchi, T.; Yamazaki, S.; Mohanty, B.; Malik, A.I.; Nagamura, Y.; Nishizawa, N.K.; Tsutsumi, N.; Colmer, T.D.; Nakazono, M. Microarray analysis of laser-microdissected tissues indicates the biosynthesis of suberin in the outer part of roots during formation of a barrier to radial oxygen loss in rice (Oryza sativa). *J. Exp. Bot.* **2014**, *65*, 4795–4806. [CrossRef]
58. Cheng, H.; Liu, Y.; Tam, N.F.Y.; Wang, X.; Li, S.Y.; Chen, G.Z.; Ye, Z.H. The role of radial oxygen loss and root anatomy on zinc uptake and tolerance in mangrove seedlings. *Environ. Pollut.* **2010**, *158*, 1189–1196. [CrossRef]
59. Armstrong, J.; Armstrong, W. Rice: Sulfide-induced barriers to root radial oxygen loss, Fe^{2+} and water uptake, and lateral root emergence. *Ann. Bot.* **2005**, *96*, 625–638. [CrossRef]
60. Armstrong, J.; Armstrong, W. Rice and Phragamites: Effects of organic acids on growth, root permeability, and radial oxygen loss to the rhizosphere. *Am. J. Bot.* **2001**, *88*, 1359–1370. [CrossRef]
61. Hose, E.; Clarkson, D.T.; Steudle, E.; Schreiber, L.; Hartung, W. The exodermis: A variable apoplastic barrier. *J. Exp. Bot.* **2001**, *52*, 2245–2264. [CrossRef] [PubMed]
62. Schreiber, L. Transport barriers made of cutin, suberin and associated waxes. *Trends Plant Sci.* **2010**, *15*, 546–553. [CrossRef] [PubMed]
63. Schreiber, L.; Franke, R.; Hartmann, K. Effect of NO_3^- deficiency and NaCl stress on suberin deposition rhizo-and hypodermal and endodermal cell walls of castor bean (*Ricinus communis* L.) roots. *Plant Soil* **2005**, *269*, 333–339. [CrossRef]
64. Ranathunge, K.; Schreiber, L.; Bi, Y.M.; Rothstein, S.J. Ammonium-induced architectural and anatomical changes with altered suberin and lignin levels significantly change water and solute permeabilities of rice (*Oryza sativa* L.) roots. *Planta* **2016**, *243*, 231–249. [CrossRef]
65. Saengwilai, P.; Nord, E.A.; Chimungu, J.G.; Brown, K.M.; Lynch, J.P. Root cortical aerenchyma enhances nitrogen acquisition from low-nitrogen soils in Maize. *Plant Physiol.* **2014**, *166*, 726–735. [CrossRef]